Type 8 Long QT Syndrome: Pathogenic Variants in *CACNA1C*-Encoded Cav1.2 Cluster in STAC Protein Binding Site

*Greg J. Mellor MB MD(Res)[1,2], *Pankaj Panwar PhD[3], Andrea K. Lee MD[1], Christian Steinberg MD[1], Julie A. Hathaway MSc[1], Kirsten Bartels MSc[1], Susan Christian MSc[4], Seshadri Balaji MBBS PhD[5], Jason D. Roberts MD[6], Chris S. Simpson MD FHRS [7], Nicole J. Boczek PhD[8], David J. Tester BS[8], Andrew E. Radbill MD[9], Ngai-Shing Mok MD[10], Robert Hamilton MD[11], Elizabeth S. Kaufman MD FHRS[12], Paul L. Eugenio MD FHRS[13], Raul Weiss MD FHRS[14], Craig January MD PhD[15], George M. McDaniel MD FHRS[16], Richard A. Leather MD[17], Christopher Erickson MD FHRS[18], Shelley Falik MD[19], Elijah R. Behr MBBS MD[20], Arthur AM Wilde MD PhD[21], Shubhayan Sanatani MD FHRS[22], Michael J. Ackerman MD PhD[8], Filip Van Petegem PhD[3], Andrew D. Krahn MD FHRS[1] , Zachary Laksman MD[1]

*These authors contributed equally.

1 Division of Cardiology, University of British Columbia, Vancouver, BC, Canada
2 Cardiology Department, Royal Papworth Hospital, Cambridge, UK
3 Department of Biochemistry and Molecular Biology, University of British Columbia, Vancouver, BC, Canada
4 Department of Medical Genetics, University of Alberta, Edmonton, Alberta, Canada
5 Dept. of Pediatrics, Division of Cardiology, Oregon Health & Science University, Portland, Oregon, USA
6 Section of Cardiac Electrophysiology, Division of Cardiology, Department of Medicine, Western University, London, Ontario, Canada.
7 Heart Rhythm Service, Division of Cardiology, Queen's University, Kingston, ON, Canada
8 Departments of Cardiovascular Medicine (Division of Heart Rhythm Services), Pediatrics (Division of Pediatric Cardiology), and Molecular Pharmacology & Experimental Therapeutics (Windland Smith Rice Sudden Death Genomics Laboratory), Mayo Clinic, Rochester, Minnesota, USA
9 Vanderbilt University Medical Center, Nashville, TN, USA
10 Department of Medicine & Geriatrics, Princess Margaret Hospital, Kowloon, Hong Kong
11 Pediatrics and Translational Medicine, University of Toronto, Toronto, ON, Canada
12 MetroHealth Campus, Case Western Reserve University, Cleveland, OH, USA
13 Division of Cardiology, Mount Sinai Hospital, New York, NY, USA
14 Wexner Medical Center, The Ohio State University, OH, USA
15 School of Medicine and Public Health, University of Wisconsin-Madison, WI, USA
16 Division of Pediatric Cardiology, University of Virginia, VA, USA
17 Royal Jubilee Hospital, Victoria, BC, Canada
18 Pediatric Cardiology, Children's Hospital & Medical Center/University of Nebraska Medical Center, NA, USA
19 Eastern Maine Medical Centre, Venice, Florida, USA
20* Cardiology Clinical Academic Group, St. George's, University of London, UK
21* Heart Centre, Department of Clinical and Experimental Cardiology, Academic Medical Centre, Amsterdam, the Netherlands
22 Children's Heart Center, BC Children's Hospital, Vancouver, BC, Canada

*Members of the European Reference Network for Rare and Low Prevalence Complex Diseases of the Heart (ERN GUARDHEART; http://guardheart.ern-net.eu)

All Authors report no conflict of interest

Short Title: CACNA1C-Mediated LQTS (LQT8)

Corresponding Author:
Zachary Laksman
1033 Davie St., Rm 211
Vancouver, BC, V6E 1M7
zlaksman@mail.ubc.ca

Keywords: Long QT syndrome, CACNA1C, ECG, genetics, 3D crystal structure

Word Count: 3581 (excluding title page, references and table/figure legends)

What's New

- The majority of LQT8-causing genetic variants cluster in a very small 'mutation hotspot' of the CACNA1C gene

- This encodes a region of the $Ca_v1.2$ protein involved in binding important regulatory STAC proteins. Altered binding of these proteins may mediate the pathogenic effects of the variants.

- Patients with these variants had a significant risk of arrhythmic events despite displaying less QT prolongation than patients with pathogenic variants in other areas of the gene

- The ECG phenotype of LQT8 displays QT prolongation after exercise similarly to LQT2.

Abstract

Aims

Pathogenic gain-of-function variants in *CACAN1C* cause type-8 Long QT syndrome (LQT8). We sought to describe the electrocardiographic features in LQT8 and utilize molecular modeling to gain mechanistic insights into its genetic culprits.

Methods

Rare variants in *CACNA1C* were identified from genetic testing laboratories. Treating physicians provided clinical information. Variant pathogenicity was independently assessed according to recent guidelines. Pathogenic (P) and likely pathogenic (LP) variants were mapped onto a 3D modeled structure of the $Ca_v1.2$ protein.

Results

Nine P/LP variants, identified in 23 patients from 19 families with non-syndromic LQTS were identified. Six variants, found in 79% of families, clustered to a 4-residue section in the cytosolic II-III loop region which forms a region capable of binding STAC SH3 domains. Therefore variants may affect binding of SH3-domain containing proteins. Arrhythmic events occurred in similar proportions of patients with II-III loop variants and with other P/LP variants (53% vs. 48%, p=0.41) despite shorter QTc intervals (477±31ms vs. 515±37ms, p=0.03). A history of sudden death was reported only in families with II-III loop variants (60% vs 0%, p=0.03). The predominant T-wave morphology was a late peaking T-wave with a steep descending limb. Exercise testing demonstrated QTc prolongation on standing and at 4 minutes recovery after exercise.

Conclusion

The majority of P/LP variants in patients with *CACNA1C*-mediated LQT8 cluster in an SH3-binding domain of the cytosolic II-III loop. This represents a 'mutation hotspot' in LQT8. A

4

late-peaking T wave with a steep descending limb and QT prolongation on exercise are

commonly seen.

Introduction

The *CACNA1C* gene encodes the core α-1 subunit of the voltage gated L-type calcium channel (LTCC) Ca$_v$1.2. *CACNA1C* is expressed in multiple cell types including cardiomyocytes. Specific variants (p.G402S and p.G406R) in exon 8, and the alternatively spliced 8A (p.G406R), were reported in the first descriptions of Timothy syndrome (TS)[1,2]. TS is a rare systemic disorder characterised by dysmorphic features, syndactyly, congenital heart disease, immune deficiency and developmental delay along with QT prolongation and an increased risk of sudden death[2]. Subsequently, additional *CACNA1C* variants outside of exon 8 have been reported in patients with non-syndromic long QT syndrome (referred to as type 8 LQTS [LQT8]) as well as in patients with: Brugada syndrome; hypertrophic cardiomyopathy, either alone or with a prolonged QT interval; and sudden unexplained death. LQT8 accounts for 1-2% of all LQTS cases. Functional assessments of LQT8-associated variants have demonstrated a gain-of-function of the LTCC through various mechanisms[3–6]. Electrocardiographic features at rest and during exercise have yet to be reported in a series of unrelated patients with *CACNA1C*-mediated LQTS. Variant distribution within the *CACNA1C*-encoded Cav1.2 and electrocardiographic phenotype at rest and during exercise are presented.

Methods

Study Population

Data from four genetic testing laboratories: GeneDx; Blueprints Genetics; the Princess Margaret Hospital Genetic Lab; and the Mayo Clinic Windland Smith Rice Sudden Death Genomics Laboratory were queried to identify patients with rare *CACNA1C* variants that were discovered between January 1, 2000 and January 31, 2017. Principal physicians in additional centers were contacted directly to identify further cases. Treating physicians were then invited to provide associated phenotypic data. Both probands and asymptomatic

relatives identified through cascade screening were included. Patients were clinically assessed by their treating physicians. Only patients with non-syndromic LQT8 were included. Patients with other phenotypes including neurological effects suggestive of Timothy Syndrome were not included. The study protocol was approved by the Research Ethics Board at the University of British Columbia.

Variant Classification

All variants classified as: pathogenic (P); likely pathogenic (LP); or of uncertain significance (VUS) by the reporting lab were originally included. Patients with P/LP variants in other LQTS or Brugada syndrome-susceptibility genes were excluded (n=1). All variants were assessed independently by three authors (GM, KB, NB) as per the 2015 American College of Medical Genetics (ACMG) guidelines[7]. The variants were annotated according to reference sequence NM_000719.6. The Exome Aggregation Consortium and Genome Aggregation Databases were used to identify general population frequencies. *In silico* pathogenicity prediction was performed using the Combined Annotation Dependent Depletion (CADD) algorithm. Public access databases were interrogated in November 2017. In addition, results of homology modelling and structural analysis (see below) were considered in variant classification. Sequence-based analyses of variants do not take into account the 3D environment of amino acid residues, which may have an important impact on function. Variants affecting residues that are buried or at an interface with another protein are more likely to be pathogenic. We therefore mapped the variants on to a 3D model of $Ca_V1.2$. Variants identified as locating to domains critical to protein function or clustering in a mutation hotspot were assigned a moderate evidence of pathogenicity criterion (designated PM1) as per the guideline recommendation[7]. Phenotypic data analysis was restricted to patients with non-syndromic LQTS and a *CACNA1C* P/LP variant.

Homology Modeling and Structural Analysis

Since no structure is available for the entire $Ca_V1.2$ complex, the three-dimensional model for human $Ca_V1.2$ was built using the cryo-electron microscopy (cryo-EM) structure of $Ca_V1.1$ complex[8] (PDB ID: 6BYO as a template, with the exclusion of cytosolic loops that are intrinsically disordered). PHYRE2 server was used for the structural modeling of $Ca_V1.2$ α_1c subunit. The overall sequence identity is 58% (69% sequence similarity), but upon exclusion of the flexible areas, which were not modeled, the overall sequence identity is 75% (86% sequence similarity), allowing for the construction of a reliable model. A sequence alignment between template and target model is shown in supplementary Figure S1. Quality control analysis by the PROCHECK program identified 93% residues of the model in the most favorable regions of the Ramachandran plot. P/LP variants were mapped on to the structure using the UniProt Q13936-12 sequence, corresponding to the NM_000719 transcript. The structural model of the $Ca_V1.2$ 851–860 peptide and STAC2 (SH3 and cysteine rich domain 2) tandem SH3 domains complex was built using the crystal structure of STAC2-$Ca_V1.1$ II-III loop complex (PDB ID: 6B27)[9]. To further investigate the contribution of the II-III loop variants on binding, we calculated the contribution of each amino acid residue within the binding site to overall binding affinity using analysis by PISA (https://www.ebi.ac.uk/pdbe/pisa/)[10]. All the structural figures were prepared and analyzed using Pymol (The PyMOL Molecular Graphics System, Version 1.8 Schrödinger, LLC.).

Phenotypic Assessment

Site investigators provided clinical data and reports of resting and exercise ECGs. Original ECG traces were provided where available. Measurements of the QT intervals were made manually using the maximum slope technique, also known as the tangent method, from 12-lead ECG recordings (25mm/s, 0.1mV/mm). Bazett's formula was used for heart rate

correction. T wave morphology was inspected visually. T wave notching was recorded if two discrete peaks were seen within the T wave. The ratio of the QT_{peak}/QT_{end} was used to quantify relative timing of QT_{peak}. Low volume T waves were defined where the peak T wave amplitude was ≤0.1mV. Where an exercise treadmill test was performed, QTc, heart rate (HR), and T-wave morphology details were recorded while: supine resting; immediately on standing; at peak exercise; at 1 minute into recovery; and at 4 minutes into recovery.

Statistical Analysis

Baseline characteristics were described using means with standard deviations. Continuous variables were compared using the Students t-test. Categorical variables were compared using the Chi-squared test. A 2-tailed P value of <0.05 was considered significant.

Results

Genetic Variant Assessment

Initially, 21 unique *CACNA1C* variants in 38 individuals from 30 families were identified from laboratory reports. Following pathogenicity assessment and evaluation of clinical data, 9 variants identified in 23 patients from 19 families with a non-syndromic LQTS phenotype were classified as either pathogenic (P, n=6) or likely pathogenic (LP, n=3) (see table 1). The remaining 12 variants (see supplemental material) were either non-pathogenic (n=10) and/or associated with phenotypes other than non-syndromic LQTS (n=6) and were not further investigated. Homology modelling and structural analysis (see below) contributed a moderate evidence of pathogenicity criterion (PM1) for one variant (p.Ala1154Val, [LP]) due to its presence in a functional domain. In addition, six of the nine (67%) P/LP variants (p.P857R, p.P857L, p.R858H, p.R860G, p.R860Q, p.R860P) identified in 15 (79%) families, were noted to cluster to a 4-amino acid long section (857-860) of the $Ca_V1.2$ protein. These variants were considered to reside in a mutation hotspot and were therefore also assigned a moderate evidence of pathogenicity criterion (PM1).

Mapping of variants on 3D protein structures

The main $Ca_V1.1$ subunit ($Ca_V\alpha_1s$) consists of a ~2000 amino acid polypeptide, with 24 transmembrane helices arranged in 4 repeats (I-IV). Each repeat contains 6 transmembrane helices (S1-S6), along with additional pore helices, whereby S1-S4 constitute a voltage sensing domain (VSD), and S5-S6 contribute to the pore. These 4 repeats are linked by long cytosolic linkers (termed I-II loop, II-III loop, and III-IV loop), and followed by a very long C-terminal cytosolic segment.

Several cytosolic loops are highly flexible and thus missing from the model, but additional high-resolution crystal structures are available for: the Cavβ subunit bound to its interaction site in the I-II loop[11–13]; for calmodulin bound to the IQ domain in the channel's proximal C-terminus[14]; and for STAC (SH3 and cysteine rich domain) proteins bound to the II-III loop of $Ca_V1.1$[9]. These allowed us to extend the structural analysis to portions not covered by the $Ca_V1.1$ cryo-EM structure.

Figure 1 shows the homology model, with the variants mapped and labeled. As described above, 6 variants (p.P857R, p.P857L, p.R858H, p.R860G, p.R860Q and p.R860P) localize to a small proline-rich region within the II-III loop. This region forms a motif recognized by SH3 domains, and the corresponding area in $Ca_V1.1$, which shows a high degree of sequence conservation with $Ca_V1.2$, forms a binding site for an SH3 domain in STAC proteins[9] (Figure 1E). STAC proteins have been shown to bind to the $Ca_V1.2$ II-III loop in vitro[9] and to affect the channel inactivation properties[9,15,16]. Recently, STAC2 was shown to be expressed in cardiac tissue[16]. The location of the variants right at the interface with the first SH3 domain of STAC2 implies they are likely to decrease affinity. The PISA analysis shows the largest contributions to binding stability are made by Pro857 and Arg858, two residues targeted by the P/LP variants in the patient cohort. Arg858 is of particular importance, as this residue makes cation-π interactions with a Trp in STAC2 and makes several salt bridge interactions.

A third residue, Arg860, is harder to interpret, since the corresponding residue in $Ca_V1.1$ was flexible in most molecules of the asymmetric unit in the STAC2 complex. However, since the STAC2 structure only covered the tandem SH3 domains, and not the N-terminal regions, this residue may interact with portions not crystallized. Therefore, it remains to be tested whether variants affecting Arg860 affect binding of STAC or other SH3-domain containing proteins.

Three variants are located within the transmembrane region. The p.G402S variant is at the C-terminal end of Repeat I S6. It has been linked previously to TS[2], and has been proposed to interfere with the mobility of the I-II loop[17]. The p.A1154V variant is located within transmembrane segment S6 of repeat III and faces the ion permeation pathway. As a result, it has the potential to interfere with Ca^{2+} flux. As S6 is also involved in the opening/closure of the intracellular gate, p.A1154V may also have an effect on gating. One cytosolic variant (p.R518H) is located in the S0 of repeat II. This loop forms a binding site for the $Ca_V\beta$ subunit, but the residue is downstream of the interaction site, and is thus not likely to impact binding directly. However, p.R518H-containing calcium channels have an in vitro gain-of-function electrophysiological phenotype[3].

Phenotypic Assessment

The mean age of the cohort was 28.3±19.4 years. 16 (70%) were probands, of whom 11 (69%) were symptomatic. The remaining 7 (30%) were relatives identified through cascade genetic testing following a familial diagnosis of LQT8 (n=6) or a sudden unexplained death event with a positive molecular autopsy (n=1).

The mean QTc on the resting 12-lead ECG of the 23 patients with P/LP variants was 487±36 ms. A late peaking T wave ($QT_{peak}/QT_{end} \geq 0.75$) with a steep descending limb was the predominant T wave morphology, observed in 15/18 (83%) patients where original ECG

traces were available. The mean QT_{peak}/QT_{end} was 0.80±0.06 (see Figure 2). A minority of patients (n=2) displayed low amplitude notched T waves.

Prior syncope or aborted sudden cardiac arrest had occurred in 11 of 23 (48%) patients. All patients with cardiac arrest (n=3) and 6/8 (75%) patients with syncope had variants in the II-III cytosolic loop. However, there was no statistically significant difference in symptomatic presentation between those patients with II-III cytosolic loop-localizing variants and those patients with variants that localized to other regions of the channel: Three out of 17 (17.6%) patients with II-III cytosolic loop variants had a cardiac arrest and 6 out of 17 (35%) had a prior syncopal event compared to none of the 6 (0%, p=0.54) and 2 out of 6 (33%. p=1.0) individuals with other pathogenic variants, respectively. There was a history of sudden unexplained death (SUD) below 30 years of age in 9 (47%) families. A history of SUD was only reported in families with II-III loop variants (60%vs. 0%, p=0.03). Mean QTc was similar in symptomatic and asymptomatic patients (491±33ms vs. 489±43ms, p=0.79). However, resting QTc measurements in patients with variants in the II-III cytosolic loop (n=17) were shorter than in patients with other P/LP (n=6) variants (477±31ms vs. 515±37ms, p=0.03). Clinical characteristics are summarized in Table 2. Individual patient data is presented in supplemental table S2.

Exercise ECGs

An exercise ECG was performed in 17 (74%) patients. The mean QTc when supine pre-exercise was 463±23ms. QTc prolongation was seen upon standing (489±53ms) and late in recovery after exercise (479±36ms) (See Figure 3). There were insufficient numbers to compare exercise test results in those with and without II-III loop variants.

Discussion

Splawski *et. al.* first described TS associated with *CACNA1C* variants in 2004[1]. Subsequently, there have been multiple cases reported of non-syndromic LQTS (LQT8) with pathogenic variants in *CACNA1C* outside of the canonical exon 8/8A[4–6,18]. This study represents the largest cohort of patients with LQT8 to date. Analysis of this cohort has allowed identification of common themes both in terms of phenotype and underlying genotype.

Genotype and 3D Protein Modelling

A striking observation from this study is that 67% of P/LP variants are tightly clustered in four consecutive amino acid residues of a protein which is 2000 amino acids in length. Furthermore, variants in this region were over-represented in the cohort, identified in 79% of families. The p.R858H variant alone was seen in 8 unrelated individuals. In addition, several of the variants from within this region have previously been reported in LQT8 patients, both by authors within this group (P857R[4], P857L[4]) and elsewhere (R858H[19], R860G[6]). Finally, data from the genome Aggregation Database shows that the sum frequency of alleles with missense/nonsense variants in amino acids 857-860 in the general population is low, at 5.67×10^{-5}, further supporting this region as a relative 'mutation hotspot' in *CACNA1C*.

The availability of several structures relating to $Ca_V1.2$ and its subunits, along with a cryo-EM structure of full-length $Ca_V1.1$, allowed us to map pathogenic variants on to a 3D model. The mutation hotspot lies in a region 10 residues (amino acid 851 to 860) long found in the cytosolic II-III loop. Functional studies in three of the previously reported variants in this region have shown a gain-of-function effect. Fukuyama *et. al*. identified the p.R858H variant in 3 unrelated cases of previously genotype negative LQTS[5]. Patch-clamp assays showed an increase in current density in p.R858H cells compared to wild-type[5]. Wemhöner *et. al.* performed patch-clamp testing on the p.R860G variant and showed a positive shift in voltage

dependence of inactivation[6]. Boczek *et. al.* identified the p.P857R variant in a 3-generation pedigree of previously genotype negative LQTS[4]. In vitro cell models demonstrated an increase in I_{CaL} and increased cell surface expression of $Ca_V1.2$. It was hypothesised that since the II-III loop contains a PEST domain (a sequence motif rich in proline [P], glutamic acid [E], serine [S] and threonine[T]) known to act as part of the signalling cascade for protein degradation, variants interrupting this sequence may lead to increased membrane stability of the channel[4]. This would lead to an increased number of functioning channels which in turn could be responsible for the increased current causing prolongation of the action potential duration and risk of early after depolarizations. More recently, it has been shown that this region contains a predicted SH3-domain binding motif, and indeed was shown to bind to SH3 domains in STAC proteins[9], a relatively recently described family of adapter proteins that have been shown to associate with $Ca_V1.1$ and $Ca_V1.2$. STAC proteins can modulate membrane trafficking and slow down channel inactivation[9,15,20]. In skeletal muscle, this interaction site is crucial for excitation-contraction coupling and is targeted by a mutation causing Native American Myopathy. Neuronal tissue expresses both STAC1 and STAC2, where they may interact with $Ca_V1.2$. STAC2 expression has recently been demonstrated in cardiomyocytes[16], however it remains to be confirmed whether it associates with $Ca_V1.2$ in these cells. In addition, SH3 domains are commonly found in a large range of proteins including the cardiac protein BIN1, which is crucial for normal $Ca_V1.2$ expression[21]. This opens the possibility that these variants are also at an interface for another SH3-domain containing binding partner. Clustering of pathogenic variants in this region, particularly affecting residues which are shown to affect binding affinity, may suggest that their pathogenic mechanism may be due to altered binding of such a partner, as an alternative, or in addition to effects on the PEST domain. Further work is needed to elucidate the identities of additional SH3-domain containing proteins that may affect $Ca_V1.2$ function.

Phenotype

Phenotype-genotype correlation is well established in the three canonical subtypes of LQTS with triggers for arrhythmic events, prognosis, response to beta-blockade and T wave morphology all varying in LQT1-3. Largely this phenotypic difference is explained by the underlying ionic culprits, with LQT1 (reduction in I_{Ks} repolarizing current), LQT2 (reduction in I_{Kr} repolarizing current) and LQT3 (increased I_{Na} depolarizing current) displaying unique clinical features.

We therefore aimed to identify common phenotypic features in LQT8. The dominant T wave morphology was a late peaking T wave with a steep descending limb, similar to classic descriptions of asymmetric late-peaking T waves in LQT3 which is also caused by an excess or prolonged depolarizing current. Changes in QT duration during exercise and recovery also differ between genotypes, with QT prolongation on exercise having been well described in LQT1 and LQT2[22], while patients with LQT3 can have variable responses[23]. A trend toward QTc prolongation on standing and in late recovery after exercise was seen in patients with LQT8 (see Figure 3). This is similar to the response seen in LQT2[22]. However, the small numbers of patients who underwent exercise testing preclude any firm conclusions and it is currently not possible to differentiate LQT8 from other subtypes based upon ECG phenotype. Future studies, with larger numbers of patients, may demonstrate unique features.

Prior clinical events were common, as might be expected in a cohort composed largely of probands. All three patients with a prior cardiac arrest and the majority with a prior syncope had variants in the II-III cytosolic loop, despite having only mild QT prolongation. Although differences in clinical events were not statistically significantly different between groups, a family history of premature sudden death was also higher in those families with II-III loop variants. Therefore, while it is not possible to conclude that variants in this region lead to a more malignant phenotype than those localized elsewhere within the gene, it a hypothesis

which requires further evaluation. The poor correlation between absolute QT prolongation and clinical events also suggest there may be an alternative mechanism of arrhythmogenesis associated with II-III loop variants in CACNA1C. The variant p.P857L has previously been reported in three unrelated individuals amongst a cohort of 174 cardiac arrest survivors without a clear phenotype undergoing genetic testing[24]. In addition, a recent report of a large family with the p.R858H variant demonstrated similar discordance between arrhythmic events and QT prolongation[25]. The authors even conclude the term 'arrhythmogenic channelopathy' may be more appropriate than LQTS in this family. Further investigation of the mechanism of arrhythmogenesis are required in addition to prospective studies to judge the prognosis of $Ca_v1.2$ II-III-loop variants and their response to treatment, which we were unable to assess. For now, it appears clear that the cytosolic II-III loop is a vital regulatory region of the $Ca_v1.2$ protein, and genetic variants affecting this area are likely to be pathogenic.

Study Limitations

The limitations to this study are inherent to a relatively small observational case series involving multiple centers. Only a portion of patients had exercise treadmill tests performed and did not routinely have treadmill tests performed both before and after the initiation of beta-blockers. The data was also collected at each participating center individually and the analysis of the resting and exercise ECG parameters was not standardized or blinded. Functional studies supporting pathogenicity were not available for all variants described.

Conclusions

We have identified a novel mutational hotspot in *CACNA1C*-encoded $Ca_v1.2$ associated with non-syndromic LQT8. The majority of pathogenic/likely pathogenic variants in $Ca_v1.2$ in patients with LQT8 cluster in a small region in the cytosolic II-III loop that can bind SH3 domains. Associated arrhythmic event rates were similar to variants elsewhere despite shorter

16

QTc intervals. The predominant T-wave morphology was a late peaking T-wave with QT prolongation on exercise.

Bibliography

1.   Splawski I, Timothy KW, Sharpe LM, Decher N, Kumar P, Bloise R, *et al.* CaV1.2 Calcium Channel Dysfunction Causes a Multisystem Disorder Including Arrhythmia and Autism. *Cell* 2004;**119**:19–31.

2.   Splawski I, Timothy KW, Decher N, Kumar P, Sachse FB, Beggs AH, *et al.* Severe Arrhythmia Disorder Caused By Cardiac L-type Calcium Channel Mutations. *Proc Natl Acad Sci* 2005;**102**:8089–96.

3.   Boczek NJ, Ye D, Jin F, Tester DJ, Huseby A, Bos JM, *et al.* Identification and Functional Characterization of a Novel CACNA1C-Mediated Cardiac Disorder Characterized by Prolonged QT Inetrvals With Hypertrophic Cardiomyopathy, Congenital Heart Defects, and Sudden Cardiac Death. *Circ Arrhythmia Electrophysiol* 2015;**8**:1122–32.

4.   Boczek NJ, Best JM, Tester DJ, Giudicessi JR, Middha S, Evans JM, *et al.* Exome Sequencing and Systems Biology Converge to Identify Novel Mutations in the L-Type Calcium Channel, CACNA1C, Linked to Autosomal Dominant Long QT Syndrome. *Circ Cardiovasc Genet* 2013;**6**:279–89.

5.   Fukuyama M, Wang Q, Kato K, Ohno S, Ding WG, Toyoda F, *et al.* Long QT syndrome type 8: Novel CACNA1C Mutations Causing QT Prolongation and

Variant Phenotypes. *Europace* 2014;**16**:1828–37.

6.   Wemhöner K, Friedrich C, Stallmeyer B, Coffey AJ, Grace AA, Zumhagen S, *et al.* Gain-of-Function Mutations in the Calcium Channel CACNA1C (Cav1.2) Cause Non-syndromic Long-QT But Not Timothy Syndrome. *J Mol Cell Cardiol* 2015;**80**:186–95.

7.   Richards S, Aziz N, Bale S, Bick D, Das S, Gastier-Foster J, *et al.* Standards and Guidelines for the Interpretation of Sequence Variants: A Joint Consensus Recommendation of the American College of Medical Genetics and Genomics and the Association for Molecular Pathology. *Genet Med*; 2015;**17**:405–23.

8.   Wu J, Yan Z, Li Z, Qian X, Lu S, Dong M, *et al.* Structure of the Voltage-gated Calcium Channel Cav1.1 at 3.6 Å Resolution. *Nature*; 2016;**537**:191–6.

9.   Wong King Yuen SM, Campiglio M, Tung C, Flucher BE, Petegem F Van. Structural Insights into Binding of STAC Proteins to Voltage-gated Calcium Channels. *Proc Natl Acad Sci* 2017;**114**:E9520–8.

10. Krissinel E, Henrick K. Inference of macromolecular assemblies from crystalline state. *J Mol Biol*; 2007;**372**:774–97.

11. Petegem F Van, Clark KA, Chatelain FC, Minor Jr DL. Structure of a Complex Between a Voltage-gated Calcium Channel β-subunit and an α-Subunit Domain. *Nature*; 2004;**429**:671.

12. Opatowsky Y, Chen C-C, Campbell KP, Hirsch JA. Structural Analysis of the Voltage-Dependent Calcium Channel Beta Subunit Functional Core and Its Complex with the Alpha-1 Interaction Domain. *Neuron*; 2018;**42**:387–99.

13. Chen Y, Li M, Zhang Y, He L, Yamada Y, Fitzmaurice A, *et al.* Structural Basis of the α1–β Subunit Interaction of Voltage-gated Ca2+ channels. *Nature*; 2004;**429**:675.

14. Petegem F Van, Chatelain FC, Minor DL. Insights into Voltage-gated Calcium

Channel Regulation from the Structure of the Ca(V)1.2 IQ Domain–
Ca(2+)/Calmodulin Complex. *Nat Struct Mol Biol* 2005;**12**:1108–15.

15.   Campiglio M, Costé de Bagneaux P, Ortner NJ, Tuluc P, Petegem F Van, Flucher BE.
STAC Proteins Associate to the IQ Domain of CaV 1.2 and Inhibit Calcium-
Dependent Inactivation. *Proc Natl Acad Sci*; 2018;**115**:201715997.

16.   Niu J, Dick IE, Yang W, Bamgboye MA, Yue DT, Tomaselli G, *et al.* Allosteric
regulators selectively prevent Ca2+-feedback of CaV and NaV channels. *Elife*
2018;**7**:1–31.

17.   Barrett CF, Tsien RW. The Timothy Syndrome Mutation Differentially Affects
Voltage- and Calcium-dependent Inactivation of CaV1.2 L-type Calcium Channels.
Proc Natl Acad Sci 2008;**105**:2157 LP – 2162.

18.   Landstrom AP, Boczek NJ, Ye D, Miyake CY, la Uz CM De, Allen HD, *et al.* Novel
Long QT Syndrome-Associated Missense Mutation, L762F, in CACNA1C-encoded
L-type Calcium Channel Imparts a Slower Inactivation tau and Increased
Sustained and Window Current. *Int J Cardiol*; 2016;**220**:290–8.

19.   Fukuyama M, Ohno S, Wang Q, Kimura H, Makiyama T, Itoh H, *et al.* L-Type
Calcium Channel Mutations in Japanese Patients With Inherited Arrhythmias. *Circ
J* 2013;**77**:1799–806.

20.   Campiglio M, Flucher BE. STAC3 Stably Interacts Through its C1 Domain with
Ca(V)1.1 in Skeletal Muscle Triads. *Sci Rep*; 2017;**7**:41003.

21.   Hong TT, Smyth JW, Gao D, Chu KY, Vogan JM, Fong TS, *et al.* BIN1 localizes the L-
type calcium channel to cardiac T-tubules. *PLoS Biol* 2010;**8**:e1000312.

22.   Sy RW, Werf C van der, Chattha IS, Chockalingam P, Adler A, Healey JS, *et al.*
Derivation and Validation of a Simple Exercise-based Algorithm for Prediction of
Genetic Testing in Relatives of LQTS Probands. *Circulation* 2011;**124**:2187–94.

23. Horner JM, Horner MM, Ackerman MJ. The Diagnostic Utility of Recovery Phase QTc During Treadmill Exercise Stress Testing in the Evaluation of Long QT Syndrome. *Hear Rhythm* 2011;**8**:1698–704.

24. Mellor G, Laksman ZWM, Tadros R, Roberts JD, Gerull B, Simpson CS, *et al.* Genetic Testing in the Evaluation of Unexplained Cardiac Arrest: From the CASPER (Cardiac Arrest Survivors with Preserved Ejection Fraction Registry). *Circ Cardiovasc Genet* 2017;**10**:10e001686.

25. Gardner RJM, Crozier IG, L. BA, Love DR, Lehnert K, Gibson K, *et al.* Penetrance and expressivity of the R858H CACNA1C variant in a five - generation pedigree segregating an arrhythmogenic channelopathy. *Mol Genet Genomic Med* 2018;1–12.

Tables and Figures

Variant No.	c.DNA Change	Amino Acid Change	Protein Topology	No. of individuals	No. of families	Variant Classification	Evidence of Pathogenicity
1	c.1204G>A	p.Gly402Ser	Rpt I S6	1	1	Pathogenic	PS3, PM1, PM2, PP2, PP3
2	c.1553G>A	p.Arg518His	I-II cytosolic loop	4	2	Pathogenic	PS3, PS4-M, PM2, PP1, PP2, PP3,
3	c.2570C>G	p.Pro857Arg	II-III cytosolic loop	1	1	Pathogenic	PS3, **PM1***, PM2, PP1, PP2, PP3,
4	c.2570C>T	p.Pro857Leu	II-III cytosolic loop	3	3	Pathogenic	PS1, **PM1***, PM2, **PM5***, PP1, PP2, PP3,
5	c.2573G>A	p.Arg858His	II-III cytosolic loop	8	8	Pathogenic	PS3, **PM1***,PM2, PP2, PP3,
6	c.2578C>G	p.Arg860Gly	II-III cytosolic loop	1	1	Pathogenic	PS3, **PM1***, PM2, PP2, PP3,
7	c.2579G>A	p.Arg860Gln	II-III cytosolic loop	3	1	Likely Pathogenic	**PM1***, **PM5***, PP2, PP3
8	c.2579G>C	p.Arg860Pro	II-III cytosolic loop	1	1	Likely Pathogenic	**PM1***, PM2, **PM5***, PP2, PP3
9	c.3461C>T	p.Ala1154Val	Rpt III S6	1	1	Likely Pathogenic	**PM1***, PM2, PP2, PP3,

Table 1. Pathogenic/likely pathogenic variants identified with ACMG 2015 guideline criteria for pathogenicity. Based upon reference sequence NM_000719.6. Asterisks denote evidence arising directly from this investigation.

	Overall Cohort	II-III loop variants	Other pathogenic variants	p
n (%)	23 (100)	17 (74)	6 (26)	-
Age (SD)	28.3 (19.4)	28.4 (16.7)	28.2 (27.6)	0.98
Male (%)	12 (52)	10 (59)	2 (33)	0.28
Proband	16 (69)	12 (71)	4 (67)	0.86
Relative	7 (31)	5 (29)	2 (33)	
Prior Symptoms	11 (48)	9 (53)	2 (33)	0.41
Prior VF	3 (13)	3 (18)	0 (0)	0.27
Prior Syncope	8 (35)	6 (35)	2 (33)	0.93
Family history of SUD ≤30 years	9 (47)*	9 (60)*	0 (0)*	0.03
QTc (SD)	487 (36)	477 (31)	515 (37)	0.03
QTp/QT (SD)	0.80 (0.06)	0.80 (0.06)	0.84 (0.07)	0.38

Table 2. Clinical characteristics stratified by site of pathogenic variant. *Proportions based upon number of families included. N_{total}=19, $n_{II-II loop}$=15 , n_{other}=4. *LQTS=Long QT Syndrome; SUD=Sudden Unexplained Death; VF=Ventricular Fibrillation*

Residue	Accessible surface area (ASA)	Buried surface area (BSA)	Solvation free energy (kcal/M)
Pro851	189.66	91.34	1.03
Glu852	161.46	9.45	- 0.08
Met853	182.00	81.97	2.38
Pro854	119.89	91.85	1.23
Val855	157.86	0.15	- 0.00
Gly856	34.11	15.09	0.09
Pro857	124.38	6.13	- 0.07
Arg858	187.46	158.17	- 1.05
Pro859	114.22	85.09	1.08
Arg860	226.54	0.00	0.00

Table 3. Solvent accessibility contribution of $Ca_V1.2$ residues in the $Ca_V1.2$ 851–860 peptide and STAC2 tandem SH3 domains complex model. Pro 857 and Arg858 shows negative solvation free energy, which corresponds to hydrophobic interfaces or positive protein affinity.
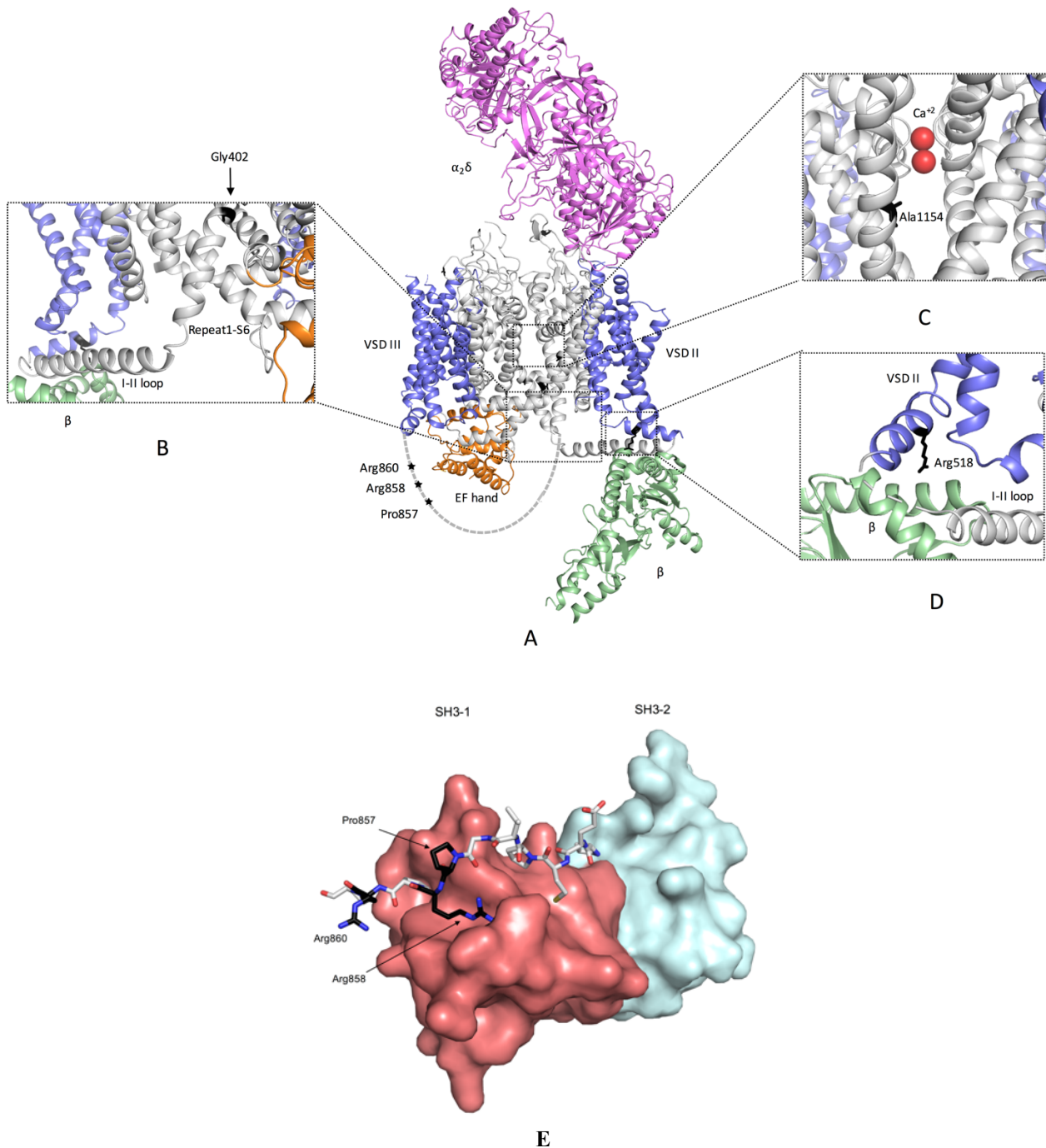
Figure 1. **Homology model of Ca$_V$1.2 complex and structural model of the Ca$_V$1.2 851–860 peptide and STAC2 tandem SH3 domains complex** (A) Ca$_V$1.2 domains are coloured as follow: α$_1$s VSD - Blue; α$_1$s pore region and cytoplasmic loops - Grey; β subunit - Light green; α$_2$δ subunit – Magenta; and α$_1$s C-terminal domain - Orange. Enlarged view of the insets are presented to highlight location of the variants and nearby secondary structures. (B) Ca$_V$1.2-p.Gly402Ser mutant is located at the C-terminal end of Repeat I S6. This mutation might affect the rigidity of S6 helix, which can interfere with the mobility of the I-II loop (C) Ca$_V$1.2-p.Ala1154Val variant is located within transmembrane segment S6 of repeat III, near the calcium binding site. (D) Ca$_V$1.2-p.Arg518His is located in the S0 helix of repeat II. This mutation is in close proximity to the Ca$_V$β subunit binding site. (E) STAC2 is shown in surface representation with the first SH3 domain in red, and the second in light blue. The

Ca$_V$1.2 peptide is shown in sticks with the residues targeted by pathogenic/likely pathogenic variants in black.
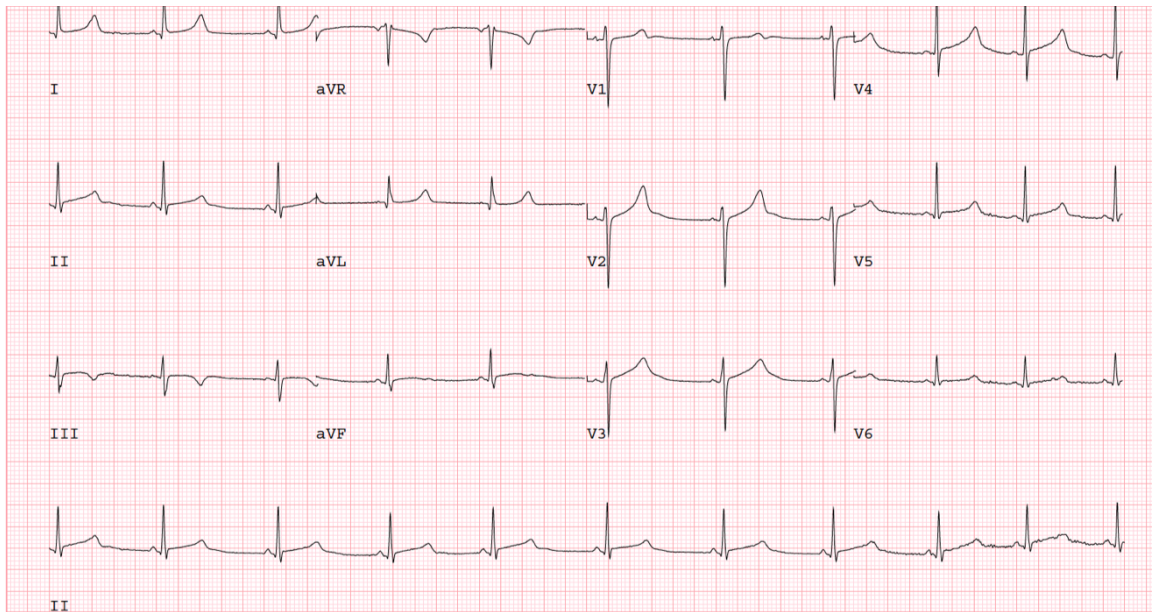

Figure 2. 12-lead ECG of Patient with R860Q variant. Note prolonged QTc with late

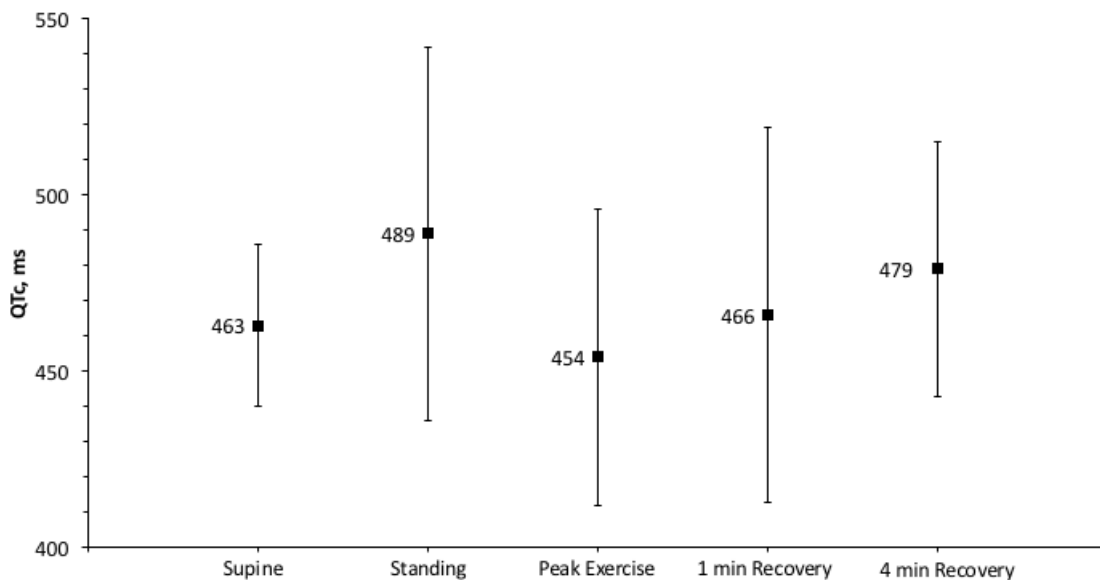peaking T wave and steep descending limb. 25mm/sec, 10mm/mV.

Figure 3. QT dynamics during exercise testing. LQT8 patients display QT prolongation on

standing and during late recovery after exercise.